AIP Advances

On the correlation of the magnetic properties with the structural parameters in Fe-doped europium chromite

Cite as: AIP Advances **11**, 035205 (2021); https://doi.org/10.1063/9.0000010
Submitted: 29 September 2020 • Accepted: 29 January 2021 • Published Online: 03 March 2021

D. R. Ratkovski, J. M. Marín Ramírez, E. L. T. França, et al.

On the correlation of the magnetic properties with the structural parameters in Fe-doped europium chromite

Cite as: AIP Advances 11, 035205 (2021); doi: 10.1063/9.0000010
Presented: 4 November 2020 • Submitted: 29 September 2020 •
Accepted: 29 January 2021 • Published Online: 3 March 2021

D. R. Ratkovski,[1] J. M. Marín Ramírez,[2] E. L. T. França,[1] A. Franco Jr.,[3] and F. L. A. Machado[1,a)]

AFFILIATIONS

[1] Departamento de Física, Universidade Federal de Pernambuco, 50670-901 Recife, Pernambuco, Brasil
[2] Instituto de Física, Facultad de Ciencias Exactas y Naturales, Universidad de Antioquia, AA 1226 Medellín, Colombia
[3] Instituto de Física, Universidade Federal de Goiás, 74690-900 Goiânia Goiás, Brazil

Note: This paper was presented at the 65th Annual Conference on Magnetism and Magnetic Materials.
[a)] **Author to whom correspondence should be addressed:** fernando.machado@ufpe.br

ABSTRACT

In the present work, the dynamics of the spins and the structural parameters of thermal treated samples of $Eu_{1-x}Fe_xCrO_3$ (x = 0, 0.1 and 0.2) were investigated. The ac-magnetic susceptibility (χ_{ac}) was measured near T_N for frequencies (f) in the range 10 - 10^4 Hz, magnitude of the ac magnetic field of 10 Oe and for $5 \leq T \leq 300$ K. X-ray diffraction data were used for determining the lattice parameters and the bonding angle θ_B (Cr– O(2) – Cr) for $100 \leq T \leq 300$ K. The maximum in χ_{ac} was found to shift to higher values of T for increasing values of f. The Vogel-Fulcher law was used for analyzing χ_{ac} yielding values for the characteristic relaxation time τ_0, activation energy E_a/k_B and glassy temperature T_G, respectively, in the ranges 2.10 - 3.96 ps, 46.5 - 47.2 K and 169.9 -176.1 K. The super-exchange parameter $J \sim \cos^4[(180 - \theta_B)/2]/d^7$, where d is the length of the bound Cr-O(2), was also obtained yielding a good correlation with the corresponding values of T_N.

I. INTRODUCTION

Multifunctional rare-earth (RE) orthochromites [RE]CrO_3 materials gained a lot of attention lately due to their potential in developing new technologies.[1–5] The orthochromites crystallize in a distorted perovskite structure with a space group Pbnm. The distortion of the ideal cubic perovskite structure actually occurs in the dodecahedral A-sites occupied by the RE-ions. The octahedron occupied by the transition metal ions (B-sites) is less distorted due to a slightly rotation.[1,6] It is also known that the magnetic properties of [RE]CrO_3 are mainly due to the antiferromagnetic (AF) interactions among the Cr^{3+} ions. The magnetic moments of the Cr^{3+} ions order in a canted antiferromagnetic (CAFM) phase showing a permanent ferromagnetic (FM) component below the Néel temperature (T_N).[7] The overall magnetic ordering is actually complex due to the presence of an isotropic super-exchange interaction and of an antisymmetric-exchange Dzyaloshinskii–Moriya (DM) coupling leading to the coexistence of CAFM with a collinear antiferromagnetic (AFM) phase.[8–17] Moreover, the occurrence of time-dependent spin-glass-like phenomena has also been reported in some perovskites.[2,3,18] Furthermore, the magnetic interactions in [RE]CrO_3 can be tuned by modifying the bond angle (θ_B) and bond length (d) associated to the Cr-O(2)-Cr interaction by replacing chromium by other transition metals.[2,3,18]

Eu^{3+} is known for having no net magnetic moment in opposite to transition metals ions. On the other hand, the large difference among their ionic radii varies the length and the angle of the bonds in the chromite $EuCrO_3$.[1,2] Thus, the influence of the addition of Fe^{3+} ions in the structure, magnetic properties and the spin dynamics of nanopowders of $Eu_{1-x}Fe_xCrO_3$, for x=0.0, 0.1 and 0.2, are investigated. The slopes of the temperature dependence of the lattice parameters were found to vary for temperatures below T_N. Additionally, the spin-dynamics yielded spin-glass-like properties that were analyzed by using the Vogel-Fulcher law. The super-exchange parameter J obtained by measuring θ_B and d was found to have a good correlation with the experimental values of T_N.

II. SAMPLES AND TECHNIQUES

Nanopowders of $Eu_{1-x}Fe_xCrO_3$ (x=0.0, 0.1 and 0.2) were synthesized by using a combustion reaction method.[2,19] The powders were then annealed for 24h at 1073K for reducing the amount of micro-strains. X-ray diffraction (XRD) was used for characterizing the structure from room temperature down to 100K by using a Rigaku Smartlab. The Maud software and the Rietveld method were employed for determining the lattice parameters and the length and the angle of the bounds. Magnetization (M) and ac-magnetic susceptibility (χ_{ac}) measurements were performed by using an ACMS modulus of a Physical Property Measurement System, made by Quantum Design, for applied magnetic fields (H) and temperatures (T), respectively, in the ranges ±85kOe and $5 \leq T \leq 300$K. The magnetization was also measured for a given value of H following two steps: (1) the sample was first cooled down to 5K under no applied magnetic field (ZFC) and (2) the sample was first cooled down to 5K with the H already applied (FC). After cooling the samples under each procedure the measurement was performed with the samples being warmed up to 300K. χ_{ac} was measured for frequencies (f) in the range $10 \leq f \leq 10^4$ Hz while keeping the ac magnetic field constant (h_{ac}=10Oe) for temperatures above and below T_N.

III. EXPERIMENTAL RESULTS

XRD spectra measured for different values of T for a non-doped sample (x=0) are shown in Fig. 1(a). It is important to call the attention to a diffraction peak near 24.3° that it is only seen below T_N. This peak is shown in details in the left-hand side inset of Fig. 1(a). Similar behavior has also been observed in other materials by either varying the sample composition or the temperature in both single-crystals and in nanoparticles, and it has been attributed to structural phase transitions induced by Jahn-Teller distortions.[20–22] Due to the thermal contraction of the sample, the diffraction peaks shift to higher values of angles as the sample is cooled down as shown in the right-hand side inset of Fig. 1(a) for the peak near 33.2°. The T-dependence of the lattice parameters (a, b and c) for the three sample concentrations (x=0.0, 0.1 and 0.2) are shown in Fig. 1(b). One may notice that the slopes of the T-dependence for the lattice parameters varies when the samples are cooled down below T_N. Interesting also that above T_N, a, b and c present nearly the same

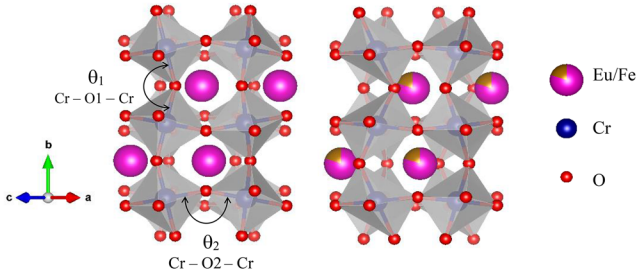

FIG. 2. Schematic drawings for the atomic distribution for x=0 (left) and x=0.2 (right). The Cr-O-Cr bond angles are also indicated. The difference in the ionic radii of Eu^{3+} and Fe^{3+} increases the distortion in the dodecahedral sites (Eu/Fe) and the rotations of the octahedrons (CrO_6).

T-dependence while below T_N the lattice parameters for the sample with x=0.1 yielded a stronger variation with T. At this point it is important to recall that the overall structural parameters depend on the degree of distortion in the sample prior the structural transition takes place. The distortions, on the other hand, are strongly influenced by the sample concentration, by the ionic distribution and on amount of micro-strains present in the samples. Thus, no simple relation with x are expected for the lattice parameters below T_N. The room temperature XRD data did also reveal that samples crystalizes into a single orthorhombic crystalline structure with space group Pbnm. These findings were used in conjunction with the VESTA software[23] to draw schematic pictures for the position of the atoms for x=0 and 0.2 (Fig. 2). The mismatch in the ionic atomic radii of Eu^{+3} (=120.6pm) and Fe^{+3} (=92pm) increases the distortion in the CrO_6 polyhedrons which, in turn, modifies the Cr-O(2)-Cr angle and the corresponding Cr-O(2) bounding length. The values of θ_B, d and the goodness-of-fitting parameter (G.O.F) are listed in Table I.

The ZFC and FC magnetizations were measured in the T-range 5–300K by applying a dc magnetic field of 100Oe showing an irreversibility for $T \leq T_N$ (Fig. 3(a)). The FC magnetization yielded a T-dependence that it is typical of ferromagnetic materials even though the net magnetization comes from the CAF induced by distortions in the CrO_6 polyhedrons. Moreover, the FC magnetization

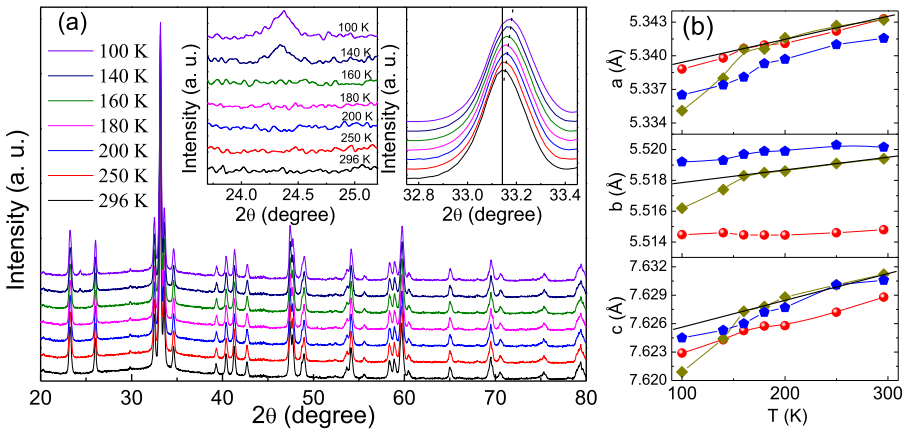

FIG. 1. (a) XRD for several values of T for a sample with x=0. The inset in the left-hand side shows a diffraction peak near 24.3 degrees that it is only seen for $T \leq T_N$. The position of the peaks shifts to higher angles for decreasing values of T as shown in the right-hand side inset for the peak near 33.2 degrees. In (b) are shown plots of the lattice parameters a, b and c vs. T for x=0 (circles), 0.1 (diamonds) and 0.2 (pentagons). The solid lines are guide to the eyes.

TABLE I. Angle and average length associated to the Cr-O(2) bond measured at room temperature.

Fe-concentration	0.0	0.1	0.2
θ_B (degree)	148.4	149.7	147.7
d (Å)	1.998	1.946	1.986
G.O.F	1.1	1.1	1.1

shows a slightly decrease below about 50K for the Fe-doped samples. This result has also been observed in others compounds[2,4,5,11] and it has been attributed to the AF-coupling of the magnetic moment of the RE^{3+} ions with the one of Cr^{3+} and to the decreasing in the average bond length RE-Cr. It was noticed that values of M were strongly influenced by the annealing that reduce the micro-strains present in the as-prepared samples.[24–26] The ZFC magnetization is substantially smaller the corresponding FC data while a kink was observed near T_N. This is somewhat expected specially in powder samples due to frozen of the magnetic moments by the local random-anisotropy.

Hysteresis loops recorded at T=5K are shown in Fig. 3(b). The magnetization data are typical of CAF with a somewhat strong FM component, e.g., non-vanishing coercivity and remanence. The FM result from the canting in the magnetic moment of the Cr^{3+} ions and from the coupling of the moments of Cr^{3+} ions with the ones of Fe^{3+} for the doped samples. The influence of the Fe-concentration in both coercivity and remanence is better seen in the inset of Fig. 3(b). Interesting, for both the coercivity and the remanence decrease for increasing values of x, a trend also found for T_N.

The dynamics of the spins was investigated by measuring χ_{ac} near T_N by varying f in the range 10-10^4 Hz. The maximum of the in-phase component of χ_{ac} was found to shift to higher values of T while the corresponding amplitude decreases for increasing values of f as shown for a non-doped sample in Fig. 4(a). This behavior is characteristic of spin-glass-like systems where the maximum shift in χ_{ac} per decade of frequency is given by $X = \Delta T/T_G[\Delta\log(f)]$,

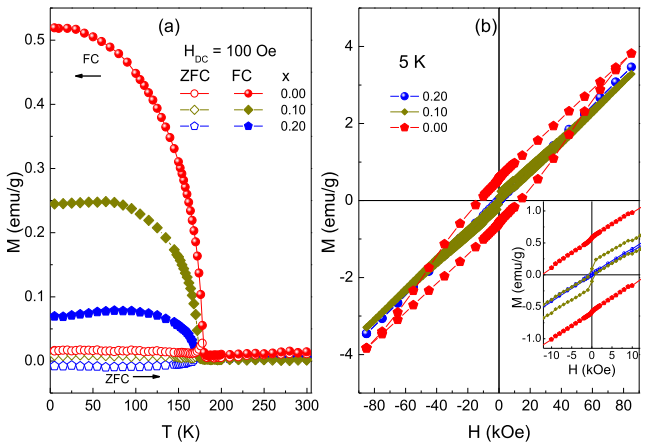

FIG. 3. (a) ZFC and FC magnetization data for a non-doped sample and (b) hysteresis loops for T=5K. The inset in (b) are blow-ups of the central part of the hysteresis loops.

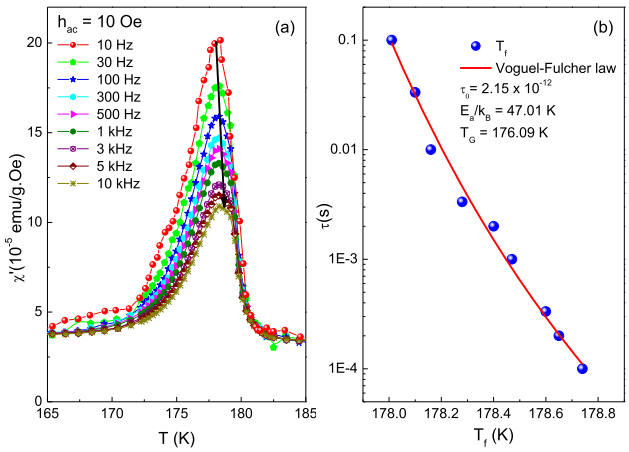

FIG. 4. (a) T-dependence of the χ_{ac} near T_N for a non-doped sample and (b) shows the correlation of T_f with τ. The solid line is a fit to the data by using the Vogel-Fulcher law.

TABLE II. Sample parameters obtained by fitting the VFL to the χ_{ac} data.

x	0.0	0.1	0.2
T_G (K)	176.1	172.5	169.9
τ_0 (10^{-12} s)	2.15	3.96	2.10
E_a/k_b (K)	47.0	47.2	46.5
X (10^{-3})	1.38	0.83	1.53

where ΔT is the variation in the temperature (T_f) at the maximum of χ_{ac} measured for the upper and lower values of f, and T_G is the glassy-temperature.[27–30] The shifting in T_f can be accounted by using the Vogel-Fulcher-law (VFL): $\tau = \tau_0 \exp\{E_a/[k_B(T_f - T_G)]\}$, where τ=1/f is the measuring time, τ_0 a characteristic relaxation time, E_a is the thermal activation energy and k_B the Boltzmann constant. Fig. 4 shows a τ vs. T_f plot for x=0 and the corresponding fitting to the VFL (solid line). The VFL was also fitted to the data for the samples with x=0.1 and 0.2 and the fitting parameters are listed in Table II.

IV. FURTHER DISCUSSIONS AND CONCLUSIONS

The super-exchange interaction is expected to be influenced by the Fe-concentration which, in turn, influences T_N ($T_N \sim J$). Along this line, J.-S. Zhou and J. B. Goodenough proposed a model for J taking into account its dependence with θ_B and d: $J \sim \cos^4[(180 - \theta_B)/2]/d^7$.[16,24,25] For instance, J is expected to increase by either increasing θ_B or decreasing d. The Zhou-Goodenough expression was used to estimate J by using the parameters measured for T (=180K), which is close but above T_N. The dependence of J with x and the correspondence of J with T_N are shown, respectively, in Fig. 5(a) and Fig. 5(b). It is important to notice the good correlation of T_N with the corresponding values of J. The dependences of θ_B and d with x are shown, respectively, in the insets (a) and (b) of Fig. 5.

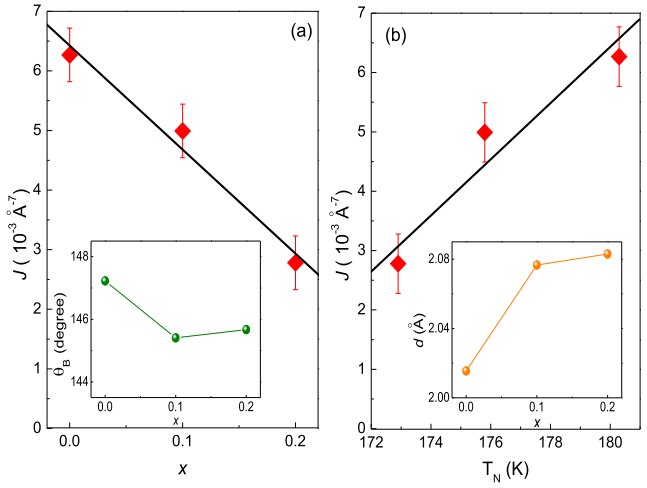

FIG. 5. (a) J calculated by using the Zhou-Goodenough model vs. x. In (b) it is shown a plot of J as function of T_N. The insets in (a) and (b) show, respectively, the dependence of θ_B and d with the iron-concentration.

In summary, nanopowders of Fe-doped europium ortho chromites were prepared and their structural and magnetic properties were investigated. The XRD data measured by varying T shown a new diffraction peak and a change in the slope in the T-dependence of the lattice parameters for values of T below T_N. θ_B and d were used to estimate de super-exchange parameter yielding a good correlation with T_N. Moreover, the addition of iron decreased the values of T_N as well as the ferromagnetic component in the canted-antiferromagnetic phase. Thus, the iron-concentration can be used for tuning the structural and the magnetic properties of europium-chromite. Finally, the χ_{ac} data showed the presence of a spin-glass-like property that was properly accounted for by the Vogel-Fulcher law.

AUTHORS' CONTRIBUTIONS

All authors contributed equally to this work.

ACKNOWLEDGMENTS

This work was partially supported by CNPq, CAPES, FACEPE and FINEP (Brazilian Agencies).

DATA AVAILABILITY

The data that support the findings of this study are available from the corresponding author upon reasonable request.

REFERENCES

[1] H. M. Widatallah, T. M. H. Al-Shahumi, A. M. Gismelseed, Z. Klencsár, A. D. Al-Rawas, I. A. Al-Omari, M. E. Elzain, A. A. Yousif, and M. Pekala, "Structural and ^{57}Fe Mössbauer study of $EuCr_{1-x}Fe_xO_3$ nanocrystalline particles," Hyperfine Interact **205**, 101–104 (2012).

[2] D. R. Ratkovski, J. M. M. Ramírez, P. R. T. Ribeiro, H. V. S. Pessoni, A. Franco, and F. L. A. Machado, "Magnetic irreversibility and spin dynamics in nanoparticles of iron-doped europium chromite," J. Alloys Compd. **724**, 501–506 (2017).

[3] M. Taheri, R. K. Kremer, S. Trudel, and F. S. Razavi, "Exchange bias effect and glassy-like behavior of $EuCrO_3$ and $CeCrO_3$ nano-powders," J. Appl. Phys. **118**, 124306 (2015).

[4] J. Prado-Gonjal, R. Schmidt, J.-J. Romero, D. Ávila, U. Amador, and E. Morán, "Microwave-assisted synthesis, microstructure, and physical properties of rare-earth chromites," Inorg. Chem. **52**, 313–320 (2013).

[5] A. Ghosh, K. Dey, M. Chakraborty, S. Majumdar, and S. Giri, "Polar octahedral rotations, cation displacement and ferroelectricity in multiferroic $SmCrO_3$," EPL **107**, 47012 (2014).

[6] T. C. Gibb, "Europium-151 Mössbauer spectra of some orthorhombic perovskites," J. Chem. Soc., Dalt. Trans. 2245–2249 (1981).

[7] K. Tsushima, I. Takemura, and S. Osaka, "Weak-ferromagnetism in $EuCrO_3$," Solid State Commun **7**, 71–73 (1969).

[8] A. H. Cooke, D. M. Martin, and M. R. Wells, "Magnetic interactions in gadolinium orthochromite, $GdCrO_3$," J. Phys. C Solid State Phys. **7**, 3133–3144 (1974).

[9] S. Lei, L. Liu, C. Wang, C. Wang, D. Guo, S. Zeng, B. Cheng, Y. Xiao, and L. Zhou, "General synthesis of rare-earth orthochromites with quasi-hollow nanostructures and their magnetic properties," J. Mater. Chem. A. **1**, 11982–11991 (2013).

[10] Y. Su, J. Zhang, B. Li, B. Kang, Q. Yu, C. Jing, and S. Cao, "The dependence of magnetic properties on temperature for rare earth $ErCrO_3$ chromites," Ceram. Int. **38**, S421–S424 (2012).

[11] T. Bora and S. Ravi, "Sign reversal of magnetization and tunable exchange bias field in $NdCr_{1-x}Fe_xO_3$ (x=0.05-0.2)," J. Magn. Magn. Mater. **386**, 85–91 (2015).

[12] B. Rajeswaran, D. I. Khomskii, A. K. Zvezdin, C. N. R. Rao, and A. Sundaresan, "Field-induced polar order at the Néel temperature of chromium in rare-earth orthochromites: Interplay of rare-earth and Cr magnetism," Phys. Rev. B **86**, 214409 (2012).

[13] H. M. Widatallah, T. M. Al-Shahumi, Z. Klencsár, M. Pekala, A. M. Gismelseed, I. A. Al-Omari, A. D. Al-Rawas, and D. Seifu, "Structural, magnetic and ^{151}Eu Mössbauer studies of mechanosynthesized nanocrystalline $EuCr_{1-x}Fe_xO_3$ particles," Acta Mater **61**, 4461–4473 (2013).

[14] V. R. Bakshi, V. P. Bandi, N. R. Gade, F. C. Chou, and S. B. Devarasetty, "Magnetization reversal in Fe doped $SmCrO_3$," Phys. Procedia. **54**, 138–144 (2014).

[15] A. A. Belik, Y. Matsushita, M. Tanaka, and E. Takayama-Muromachi, "Crystal structures and properties of perovskites $ScCrO_3$ and $InCrO_3$ with small ions at the A site," Chem. Mater. **24**, 2197–2203 (2012).

[16] A. K. Mall, A. Garg, and R. Gupta, "Modifications of the structure and magnetic properties of ceramic $YCrO_3$ with Fe/Ni doping," Mater. Res. Express. **4**, 076104 (2017).

[17] R. M. Hornreich, "Magnetic interactions and weak ferromagnetism in the rare-earth orthochromites," J. Magn. Magn. Mater. **7**, 280–285 (1978).

[18] F. Rivadulla, M. A. López-Quintela, and J. Rivas, "Origin of the glassy magnetic behavior of the phase segregated state of the perovskites," Phys. Rev. Lett. **93**, 167206 (2004).

[19] J. M. M. Ramírez, H. V. S. Pessoni, A. Franco, and F. L. A. Machado, "Synthesis of europium orthochromites ($EuCrO_3$) nanoparticles by a combustion reaction method," J. Alloys Compd. **690**, 315–320 (2017).

[20] G. Ueno, S. Sato, and Y. Kino, "The low-temperature tetragonal phase of NiCr204," Acta Cryst C **55**, 1963–1966 (1999).

[21] J. Yang, "Structural analysis of perovskite LaCr1-xNixO3 by Rietveld refinement of X-ray powder diffraction data," Acta Cryst B **64**, 281–286 (2008).

[22] I. Matulková, P. Holec, I. Nemec, H. Kitazawa, T. Furubayashi, and J. Vejpravová, "Temperature-dependent vibrational spectroscopic and X-ray diffraction investigation of nanosized nickel chromite," J. Mol. Struc. **1090**, 70–75 (2015).

[23] K. Momma and F. Izumi, "*VESTA* 3 for three-dimensional visualization of crystal, volumetric and morphology data," J. Appl. Crystallogr. **44**, 1272–1276 (2011).

[24] J.-S. Zhou and J. B. Goodenough, "Intrinsic structural distortion in orthorhombic perovskite oxides," Phys. Rev. B **77**, 2–5 (2008).

[25]J.-S. Zhou, J. A. Alonso, V. Pomjakushin, J. B. Goodenough, Y. Ren, J.-Q. Yan, and J.-G. Cheng, "Intrinsic structural distortion and superexchange interaction in the orthorhombic rare-earth perovskites RE-CrO_3," Phys. Rev. B **81**, 1–5 (2010).
[26]M. Taheri, F. S. Razavi, and R. K. Kremer, "Rare earth chromium oxides revisited, special case: Structural, magnetic and thermal studies of $Ce_{1-x}Eu_xCrO_3$ nano-powders," Phys. C Supercond. Appl. **553**, 8–12 (2018).
[27]F. L. A. Machado, F. C. Montenegro, S. M. Rezende, E. Montarroyos, L. J. Azevedo, and W. G. Clark, "Spin-glass behavior in the A1:Mn quasicrystalline alloys," Solid State Commun **79**, 469–471 (1991).
[28]P. R. T. Ribeiro, J. M. M. Ramírez, R. Vidyasagar, F. L. A. Machado, S. M. Rezende, and E. D. Dahlberg, "GMI in the reentrant spin-glass $Fe_{90}Zr_{10}$ alloy: Investigation of the spin dynamics in the MHz frequency regime," Appl. Phys. Lett. **109**, 102404 (2016).
[29]K. Vijayanandhini, C. Simon, V. Pralong, V. Caignaert, and B. Raveau, "Spin glass to cluster glass transition in geometrically frustrated $CaBaFe_{4-x}Li_xO_7$ ferrimagnets," Phys. Rev. B **79**, 224407 (2009).
[30]A. Kumar, R. P. Tandon, and V. P. S. Awana, "Successive spin glass, cluster ferromagnetic, and superparamagnetic transitions in $RuSr_2Y_{1.5}Ce_{0.5}Cu_2O_{10}$ complex magneto-superconductor," Eur. Phys. J. B. **85**, 238 (2012).